Direct Evidence for the Partial Dehydration of Phosphatidylethanolamine Bilayers on Approaching the Hexagonal Phase†

John Katsaras,*,‡ Kenneth R. Jeffrey,§ Daniel S.-C. Yang, and Richard M. Epand

Department of Biochemistry, McMaster University, 1200 Main Street West, Hamilton, Ontario L8N 3Z5, Canada

Received April 21, 1993; Revised Manuscript Received July 27, 1993®

ABSTRACT: X-ray diffraction studies on oriented multilayers of 1-palmitoyl-2-oleoylphosphatidylethanolamine (POPE) in the lamellar gel (L_β) and inverted hexagonal (H_{II}) phases at various temperatures (5–50 °C) and relative humidities (0–100%) are reported. One-dimensional electron density profiles of the L_β phase bilayers were constructed to a resolution of better than 4 Å using direct methods to solve for the phase problem. In addition, the electron density profiles were fitted favorably using a model in which the atomic groups were assumed to be Gaussian distributed [Wiener, M. C., & White, S. H. (1992) *Biophys. J. 61*, 434–447]. The X-ray data clearly demonstrate that, at 100% relative humidity (RH), POPE samples exist in two distinct L_β phases, differing primarily in the amount of water between the lamellae. As the hexagonal phase transition temperature is approached, 100% RH POPE samples partially dehydrate, releasing approximately 5 water molecules per phospholipid and experiencing on average a 3-Å decrease in repeat spacing. The lower temperature hydrated L_β phase POPE electron density distribution resembles that obtained from the L_β phase 1-palmitoyl-2-oleoylphosphatidylcholine (POPC) bilayers and is unlike the partially dehydrated POPE bilayers.

Although it has been well-known for several decades that lipid–water systems form a number of structural phases, the molecular basis of lipid polymorphism remains poorly understood. One family of lipids which can exist in a variety of structural phases within easily accessible experimental conditions is the phosphatidylethanolamines (PE's). They undergo not only the much observed gel (L_β) to liquid-crystalline (L_α) phase transitions (Seddon et al., 1984) but also well-defined transitions to nonlamellar phases such as the inverted hexagonal (H_{II}) (Gawrisch et al., 1992; Cullis & De Kruijff, 1979) and sometimes directly from the L_β to H_{II} phase, bypassing the L_α phase altogether (Marsh & Seddon, 1982). Besides providing the possibility of a polymorphic structural study, PE's are known in certain cases to form metastable phases (Seddon et al., 1984; Chang & Epand, 1983; Mantsch et al., 1983; Wilkinson & Nagle, 1981).

The effects of hydration on metastability and lipid structure have been studied by a number of investigators using a variety of techniques [e.g., Gawrisch et al. (1992), Rand et al. (1988), and Seddon et al. (1984)]. For example, PE's exhibit a markedly lower water affinity compared to phosphatidylcholines (PC's). However, a single methylation of the PE polar headgroup changes the degree of hydration to nearly that of PC (Rand et al., 1988). This tendency for a lower water affinity in PE's can probably be attributed to the strong electrostatic and hydrogen-bonding interactions that exist between PE headgroups, both in the plane of the bilayer and between adjacent bilayers (Boggs, 1987; McIntosh & Simon, 1986; Seddon et al., 1984). In addition, the L_β phase of PE's has been shown to be metastable in excess water (Epand, 1990), spontaneously dehydrating and reverting to crystalline forms within a few hours (Seddon et al., 1984). In contrast, dipalmitoylphosphatidylcholine partially dehydrates to a crystalline phase only after several days of incubation in the region of 0 °C (Chen et al., 1980; Ruocco & Shipley, 1982).

Recently, there has been considerable interest in the dehydration effects which accompany the lamellar-to-hexagonal phase transitions in lipid/water systems (Webb et al., 1993; Bryant et al., 1992; Castresana et al., 1992; Bryant & Wolfe, 1989). Biological membranes can incur dehydration-induced damage correlated to the formation of lateral phase separation and H_{II} phase formation (Crowe & Crowe, 1982; Gordon-Kamm & Steponkus, 1984). It is important to note that the formation of a hexagonal phase poses some serious biological problems to a cell membrane since, in this phase (e.g., H_{II}), it would not adequately perform as a selective barrier between the cell interior and the external environment. In biological membranes, nonbilayer phase formation is probably only a transient process and has been correlated with a number of vital biological membrane functions (Epand, 1991).

In this study using X-ray diffraction, we attempted to provide some insight into the polymorphic and possible metastable tendencies of POPE.[1] We have made systematic X-ray diffraction measurements of POPE and POPC as a function of hydration and temperature, observing the various structural phase transitions. The one-dimensional electron density maps, obtained by Fourier transforming the diffraction patterns, provide direct evidence of the partial dehydration of PE headgroups as a function of temperature at constant humidity (100% RH). This provides a picture which implies that a dehydrated L_β phase (possibly metastable) is a necessary

† This work was supported by a grant (MA-7654) from the Medical Research Council of Canada and by the Natural Sciences and Engineering Research Council of Canada (NSERC). J.K. is the recipient of an NSERC postdoctoral fellowship.

* Address correspondence to this author.

‡ Present address: Centre de Recherche Paul Pascal-CNRS, Avenue A. Schweitzer, F-33600 Pessac, France.

§ Permanent address: Department of Physics, University of Guelph, Guelph, Ontario N1G 2W1, Canada.

® Abstract published in *Advance ACS Abstracts*, September 15, 1993.

[1] Abbreviations: POPE, 1-palmitoyl-2-oleoylphosphatidylethanolamine; POPC, 1-palmitoyl-2-oleoylphosphatidylcholine; RH, relative humidity; *d*-spacing, lattice repeat spacing; DPPC, 1,2-dipalmitoylphosphatidylcholine.

0006-2960/93/0432-10700$04.00/0

precursor to the H_{II} phase, at least for $L_\beta \rightarrow H_{II}$ phase transitions.

EXPERIMENTAL PROCEDURES

Materials

POPE and POPC were obtained from Avanti Polar Lipids, Inc. (Birmingham, AL) and used as supplied. Lipid purity was checked using thin-layer chromatography (TLC; developing solvents $CHCl_3/CH_3OH/H_2O/NH_4OH$, 58:35:5.4:1.6) where a single nondiffuse spot was observed with iodine vapor.

Methods

X-ray Diffraction. POPE and POPC bilayers were oriented by placing a concentrated solution of lipid dissolved in methanol on the surface of a 30-mL Pyrex beaker which was subsequently placed in a vacuum for 24 h to remove the methanol. The lipid sample was then placed in a 100% RH environment at room temperature for 24 h. POPE samples at 100% RH used in the temperature experiment (5–50 °C) were annealed in an environment of 100% RH and 5 °C for 24 h. POPE and POPC samples used in the incremental RH experiments were dehydrated under vacuum for 24 h. Experiments in all cases were repeated with the *d*-spacings having an uncertainty of ±0.2 Å while the structure factor amplitudes contained uncertainties of up to 20% for the weakest Bragg reflections.

Two-dimensional diffraction patterns were obtained with an R-Axis IIC image plate detector (Rigaku Corp., Japan) having a pixel size of 105 × 105 μm^2 and an effective detection area of 200 × 200 mm^2 using a point source of Cu Kα radiation from a Rigaku Rotaflex RU-200B series rotating anode X-ray generator (Rigaku Corp., Japan) operating at 4 kW (50 kV and 80 mA). Monochromation of the Cu radiation was achieved using a graphite crystal. Diffraction patterns were obtained using an exposure of 30 min. The diffraction patterns were radially integrated and the intensities of the diffraction peaks determined from the pattern after background subtraction. The intensities were scaled using a half-Lorentzian correction; that is, the intensities were multiplied by the order of the diffraction peak, *h* (Franks, 1976).

The sample holder was constructed from aluminum and permitted us to monitor and adjust both the RH and temperature. The RH was monitored by a digital hygrometer and was adjusted by varying the flow rate of nitrogen gas (0% RH) or nitrogen gas through a gas washer bottle filled with water (>0% RH) before passage through the sample holder. The temperature was regulated by a water bath. Finally, the sample holder was positioned so that the X-ray beam passed through the sample tangent to the vertical curved side of the beaker.

Solution to the Phase Problem. In cases where bilayers were able to swell with increasing levels of hydration, the reflections were phased using the Shannon sampling theorem (Shannon, 1949; Sayre, 1952; Torbet & Wilkins, 1976; Katsaras & Stinson, 1990). The zeroth-order amplitude necessary for the reconstruction of the continuous Fourier transforms was calculated by subtracting the electron density of water from the average electron density of the bilayer and multiplying by the *d*-spacing (Katsaras et al., 1991). However, there are two situations which exclude the swelling method from being used successfully: (a) The lipid multilayers cannot swell, and as such the continuous transform cannot be mapped out. (b) The motif (lipid bilayer) is not preserved. The continuous transform can still be sampled at different reciprocal lattice points if the motif only undergoes small

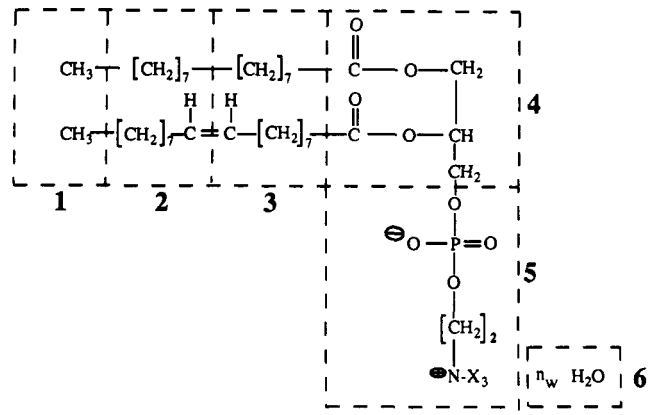

FIGURE 1: Parsing scheme used for both POPE and POPC molecules. X represents an H for PE headgroups and a CH_3 for PC headgroups.

gradual changes (e.g., increasing tilt with increasing hydration) (Torbet & Wilkins, 1976; Katsaras & Stinson, 1990). For the POPC sample at 20 °C and 0% RH, the bilayers could not be induced to swell. In addition, the POPC sample was found to undergo a phase transition at about 15% RH. Consequently, the phase problem for the L_δ phase POPC sample was solved using the triplet structure invariant relationships described in a series of publications by Dorset (1991a,b, 1990). In addition, modeling of the electron density distributions provided an added measure of confidence in the assigned phases, since the crystallographic *R*-factor was found to be a minimum when the phases agreed with those derived by the direct methods.

Modeling of the Electron Density Profile. We employed a method similar to that of Wiener and White (1992) in the reconstruction of the electron density maps. Lipid bilayers were described as a series of multiatomic quasimolecular fragments, each represented by a Gaussian distribution in composition space (Wiener & White, 1991). Figure 1 represents the parsing scheme which was successfully used for all of the POPE and POPC samples.

In a unit cell there are two lipid and a number of water molecules (n_w). The number of water molecules, n_w, is a variable in the model. Each of the six groups used has a scattering length, b_i, which is simply the sum total of the number of electrons in each group. In addition, each molecular fragment is assumed to be Gaussian distributed, centered at Z_i and having a width A_i. Since the position of the water region is assumed to be centered at $d/2$, the number of fitting parameters used was 12. The calculated scattering length profile is therefore given by

$$\rho_M(Z) = \sum_i \frac{b_i}{S\pi^{1/2}A_i} e^{-[(Z-Z_i)/A_i]^2} \quad (1)$$

while the calculated structure factors are

$$f_M(h) = \frac{2}{S}\sum_i b_i e^{-(\pi A_i h/d)^2} \cos\frac{2\pi Z_i h}{d} \quad (2)$$

where *d* is the repeat spacing and *S* is the cross section of a lipid. Since *S* is unknown, the modeling gives

$$f_m(h) = Sf_M(h) = 2\sum_i b_i e^{-(\pi A_i h/d)^2} \cos\frac{2\pi Z_i h}{d} \quad (3)$$

$f_m(h)$ are the structure factors on a relative absolute scale (Wiener & White, 1992).

Since the observed structure factors are not absolute, the experimental data were scaled. The experimental scattering

length profile (i.e., electron density distribution) is given by

$$\rho_e(Z) = \frac{f_0}{d} + \frac{2}{d}\sum_{h=1}^{h_{max}} \frac{f_e(h)}{K} \cos \frac{2\pi Zh}{d} \quad (4)$$

where f_0 is the zeroth-order structure factor and K is a scaling factor. In order to make use of eq 4, f_0 and K must be determined. The zeroth-order structure factor, f_0, was given the value determined from the model calculation, eq 3. The calculated and experimental profiles were set equal to each other at $Z = 0$, i.e.

$$\rho_e(Z=0) = \rho_M(Z=0)$$

Therefore

$$\sum_{h=1}^{h_{max}} \frac{f_e(h)}{K} = \sum_{h=1}^{h_{max}} f_m(h)$$

$$K = \frac{\sum_{h=1}^{h_{max}} f_e(h)}{\sum_{h=1}^{h_{max}} f_m(h)} \quad (5)$$

Estimates of the fitting parameters Z_i, A_i, and n_w are made, and the structure factors can be calculated since the b_i's associated with each molecular fragment are known. The model structure factors are therefore obtained by use of eq 3. A comparison of the calculated and experimental structure factors was made by calculating the residual

$$R = \frac{\sum_{h=1}^{h_{max}} |K f_m(h) - f_e(h)|}{\sum_{h=1}^{h_{max}} |f_e(h)|} \quad (6)$$

The fitting parameters A_i, Z_i, and the number of waters were determined by minimizing the residual (eq 6) using the Nelder–Meade simplex algorithm (Press et al., 1992). Typically, the R-factors were about 0.040. For the POPC bilayers at 20 °C and 0% RH a residual of 0.015 was obtained. Finally, for all data sets 13 or 14 orders were used for the fits.

Although we do not pretend that the parsing model used in this study is a unique description of either the POPE or POPC bilayers, we were encouraged to observe that one parsing scheme satisfactorily fit all 24 independent data sets. The only difficulty that we encountered was that the model was not very sensitive to the number of waters. Equally good fits were obtained with a few waters with a narrow distribution or with many waters spread widely. The best way to determine the water distribution experimentally would be from neutron diffraction experiments (Wiener et al., 1991).

RESULTS AND DISCUSSION

Electron Density Profiles for POPE Bilayers. In Figure 2, we present two-dimensional X-ray diffraction patterns for the lamellar (Figure 2a,c) and the hexagonal (Figure 2e) phases of POPE at various temperatures (20–50 °C) and 100% RH. The diffraction pattern shown in Figure 2a is for the L_β phase at 20 °C where the d-spacing is 58.0 Å. The pattern shown in Figure 2c is for the partially dehydrated L_β phase with a d-spacing of 55.0 Å, which evolves from the hydrated phase at increasing temperatures. The diffraction pattern in Figure 2b is for the L_β phase at 20 °C where the d-spacing is 58.0 Å along with a reflection corresponding to 12.5 Å, which is not part of the lamellar series and does not correspond to any of the reflections of the partially dehydrated L_β phase (Figure 2c) where the d-spacing is 55.0 Å. At present, we do not have an explanation for the 12.5-Å reflection except that it may be the result of some periodic lamellar defect formation

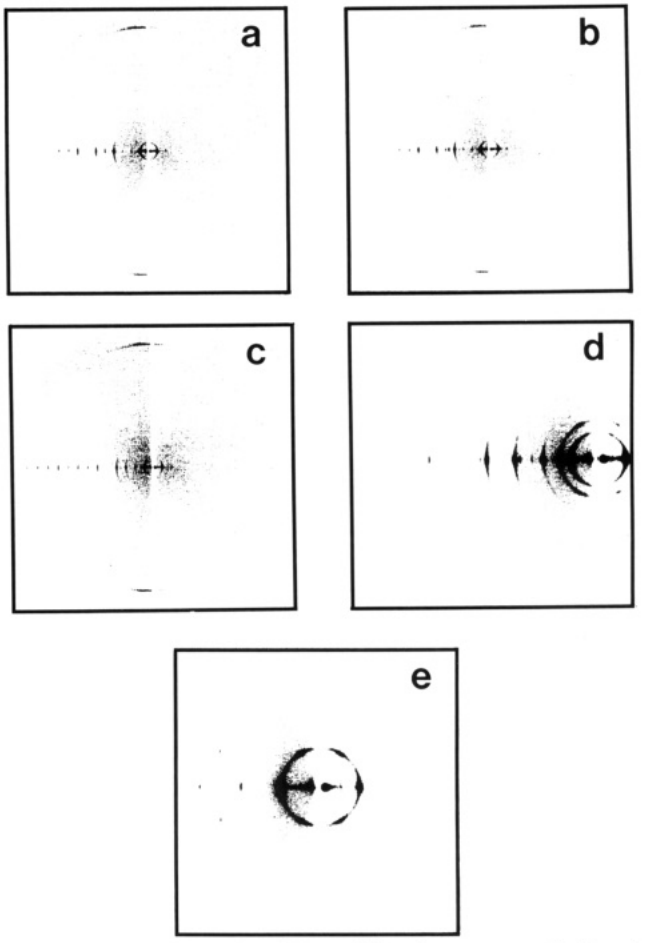

FIGURE 2: Two-dimensional X-ray diffraction patterns of oriented lamellar and hexagonal phase POPE at 100% RH. Panels: (a) L_β phase at 20 °C; (b) metastable coexistence of the L_β and partially dehydrated L_β phases at 25 °C; (c) partially dehydrated L_β phase at 30 °C; (d) metastable coexistence of the partially dehydrated L_β and H_{II} phases at 45 °C; (e) H_{II} phase with a d-spacing of 39.9 Å at 50 °C.

(Bagdassarian et al., 1991). In the transition from the L_β to partially dehydrated L_β phase at 30 °C and 100% RH (Figure 2c), a reflection with a spacing of 44.5 Å appears (Figure 2c) which also does not belong to the lamellar reflection set. At 40 °C (data not shown) the 44.5-Å reflection decreases to 39.8 Å and subsequently becomes the first order of the H_{II} phase (Figure 2d). If the phases in panels b and c of Figure 2 contain periodic defects, then the phases can be metastable. In the hexagonal phase (Figure 2e), the sharp wide-angle reflection in the 1/4.2 to 1/4.3 $Å^{-1}$ region due to the hexagonally packed hydrocarbon chains and indicative of gel phase bilayers (e.g., Figure 2a–c) is no longer present (data not shown), implying that the hydrocarbon chains of POPE in the H_{II} phase are in a fluid state (Seddon et al., 1984).

Figure 3 contains the continuous Fourier transforms reconstructed by use of the sampling theorem for the POPE bilayers at 100% RH and various temperatures. If the bilayer (motif) remains unaltered, all of the continuous Fourier transforms will superimpose upon one another if the transforms are reconstructed using the correct phase choices (Torbet & Wilkins, 1976). The continuous Fourier transforms for POPE bilayers in the temperature range from 5 to 20 °C at 100% RH, where the d-spacings lie between 57.7 and 58.0 Å, are shown in Figure 3a. In contrast to Figure 3a, we present the continuous transforms calculated for the same sample using a phase assignment of (+) instead of (–) for the sixth order (Figure 3b). As one can observe, the superposition of the

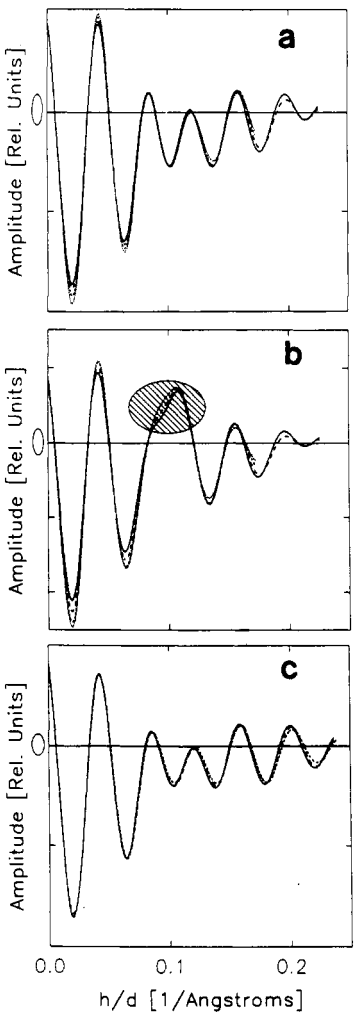

FIGURE 3: Continuous Fourier transforms of 100% RH POPE bilayers. Panels: (a) L_β phase bilayers [(—) 5 °C (57.7 Å), (– – –) 10 °C (57.7 Å), (- - -) 15 °C (58.0 Å), (···) 20 °C (58.0 Å)]; (b) same as (a) except the sixth-order phase is (+) instead of (–); (c) partially dehydrated L_β phase POPE bilayers [(—) 30 °C, (– – –) 35 °C, (···) 40 °C]. The corrected structure factors for the L_β phase bilayers from 5 to 20 °C are –3672, 541, –394, –2145, 320, –1129, 0, –1181, 459, –797, 148, 0, 140; –3647, 497, –305, –2208, 334, –1128, 0, –1135, 436, –658, 0, 0, 80; –3674, 447, –186, –2288, 367, –1127, 0, –1118, 390, –455; and –3746, 431, –145, –2342, 363, –1118, 0, –999, 322, –355, respectively. For the partially dehydrated L_β phase bilayers at 30 (55.0 Å), 35 (54.7 Å), and 40 °C (54.4 Å), the corrected structure factors are –4563, 1025, –1254, –1598, 0, –753, –443, –586, 340, –941, 551, –558, 221; –4333, 969, –1205, –1612, 0, –765, –398, –557, 350, –885, 500, –505, 213; and –4310, 989, –1231, –1463, 0, –628, –379, –438, 257, –849, 424, –399, 161, respectively.

curves in the vicinity of the sixth order (as indicated by the hatched ellipsoid) is inferior to the same region in Figure 3a. This effect can be shown using any non-zero intensity reflection. Thus, we chose the sixth-order reflection throughout since it was consistently intense in all of the samples used in this study. The same criteria as those used to determine the continuous transforms in Figure 3a were applied to the partially dehydrated L_β phase in the temperature region from 30 to 40 °C to produce the continuous transforms shown in Figure 3c.

In Figure 4 we present electron density distributions on a relative electron density scale for the 100% RH POPE bilayers at 20 (Figure 4a) and 30 °C (Figure 4b) calculated from the structure factors obtained in Figure 3. The two most obvious differences between the two distributions are at the glycerol-backbone and polar headgroup regions. There is a significant decrease in the water region (phosphate-to-phosphate separation) of the partially dehydrated L_β phase, and the peaks attributed to the backbone and headgroup are much better resolved in the 30 °C gel phase. These two features are indicative of bilayers with lesser amounts of water and have been clearly observed with DPPC bilayers at 20 °C when the amount of water was varied (Katsaras & Stinson, 1990).

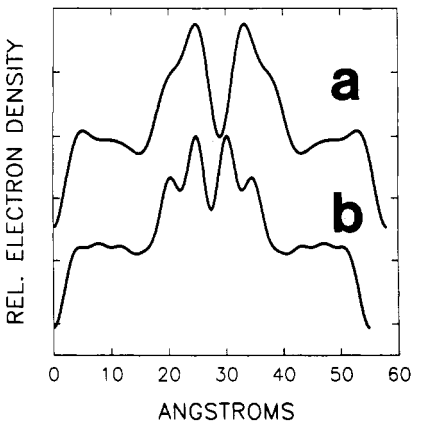

FIGURE 4: Electron density profiles of (a) 58.0-Å L_β phase POPE bilayers at 20 °C and (b) 55.0-Å partially dehydrated L_β phase POPE bilayers at 30 °C. Both profiles are of bilayers at 100% RH.

Figure 5a shows the center of the Gaussian distribution of the various multiatomic quasimolecular fragments described in Figure 1. At 30 °C, there is a definite shift to a smaller distance (i.e., smaller Z values) for all Gaussian distribution positions except those representing fragments 4 and 5 which correspond to the glycerol-backbone and polar headgroups, respectively. This implies some hydrocarbon chain reorganization, resulting in the partially dehydrated phase of POPE (30–40 °C) having an effective length which is slightly greater than that of the L_β phase lipids at temperatures ≤20 °C. Some additional evidence of this can be found in a study by Katsaras and Stinson (1990), where a DPPC + 40 mol % palmitic acid system at 20 °C and various RH's was used. Panels b and c of Figure 5 clearly demonstrate that the changes in d-spacing as a function of temperature mirror the changes in the water region. Once in the partially dehydrated L_β phase, the POPE bilayers continue to dehydrate (Figure 5c) and proceed to the H_{II} phase. However, this dehydration is on a considerably smaller scale as compared to the dehydration occurring during the L_β to partially dehydrated L_β phase transition.

Recently, a study by Castresana et al. (1992) using Fourier transform infrared (FTIR) spectroscopy observed that, in egg yolk PE at pH 5.0 and excess water conditions, the portion of the FTIR spectrum corresponding to the phosphate group revealed a weakening in the shell of hydrogen-bonded water when the lipid was undergoing a lamellar to hexagonal phase transition, indicative of a partial dehydration of the phosphate group. This was not observed in the gel-to-liquid-crystalline phase transition. Finally, in a low-hydration condition (~8 mol of water/mol of lipid) Castresana et al. observe a single transition which they correctly speculate to be an L_β to H_{II} transition. Our results agree in principle with those obtained by Castresana et al. (1992); however, we differ on the following points: (a) We observe two L_β phases differing principally in their water content. The partially dehydrated L_β phase of POPE is a precursor phase, necessary for the lipid to undergo a hexagonal phase transition and which coexists with a nonlamellar reflection over a range of 20 °C. (b) During the hexagonal phase transition we do not observe an abrupt partial dehydration of the hydrophilic headgroup but rather small gradual decreases in the size of the water region. The first

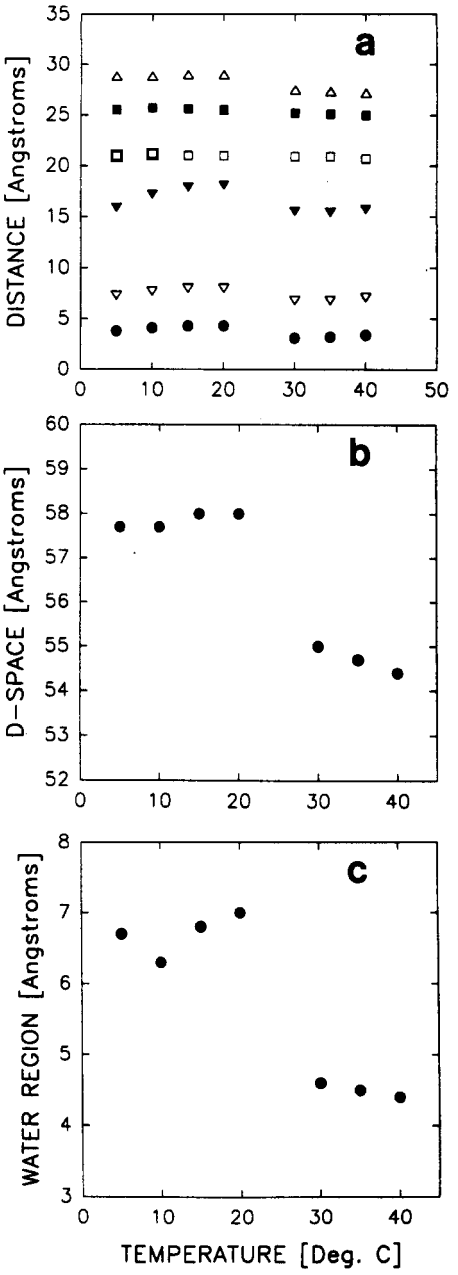

FIGURE 5: Temperature dependence at 100% RH of (a) the quasimolecular fragments (please refer to Figure 1) characterizing the structure of L_β phase (5–20 °C) and partially dehydrated L_β phase (30–40 °C) POPE [(●) 1; (▽) 2; (▼) 3; (□) 4; (■) 5; (△) 6], (b) the *d*-spacing in POPE bilayers, and (c) the water region (two times the difference between quasimolecular fragments 5 and 6).

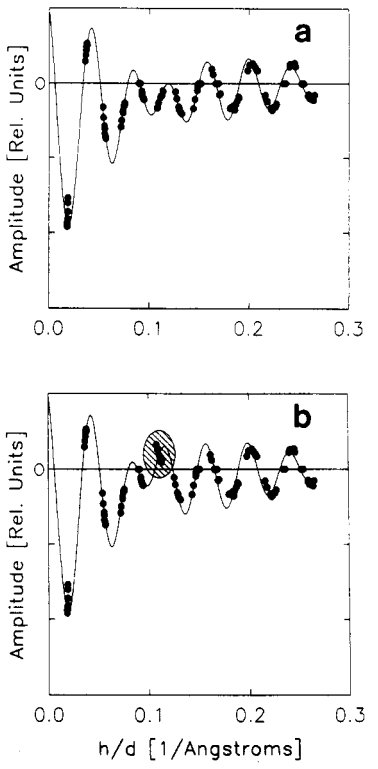

FIGURE 6: (a) Structure factors (●) obtained in a series of swelling experiments at 20 °C of partially dehydrated L_β POPE bilayers with a superimposed continuous Fourier transform (—) calculated for the 70% RH sample. (b) Same as (a) except the sixth-order phase is positive.

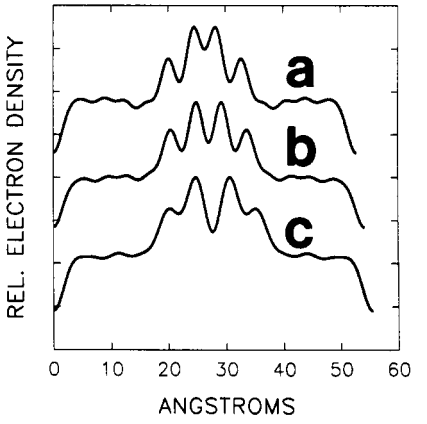

FIGURE 7: Electron density profiles of partially dehydrated L_β phase POPE bilayers at 20 °C and (a) 0% RH (*d*-spacing = 52.8 Å), (b) 70% RH (54.1 Å), and (c) 100% RH (55.5 Å).

difference can possibly be explained by the fact that we used POPE incubated at 5 °C for 24 h instead of egg PE. The second point we cannot fully explain except that Castresana et al. (1992) never give an actual number as to how many water molecules depart the headgroup site during the lamellar to hexagonal phase transition. Figure 5c shows that the phase transition between L_β phases occurring between 20 and 30 °C results in a loss of approximately 5 water molecules per lipid and is followed by a small further continuous decrease in the size of the water region above 30 °C.

Due to the unusual behavior of the electron density profiles of the partially dehydrated POPE bilayers, the question of the correct phases for the structure factors was reexamined. In Figure 6a we present the structure factors obtained from POPE bilayers at 20 °C and various RH's. As can be seen, all of the experimental structure factors are fitted by one continuous Fourier transform which was calculated for bilayers at 70% RH having a *d*-spacing of 54.1 Å. Changing the phase of the sixth order to (+) from (–) for all the conditions and recalculating the transform (Figure 6b) results in a breakdown of the fit. The signs of the structure factors (Figure 6a) are identical to those of the partially dehydrated L_β phase POPE bilayers in Figure 3c.

Figure 7 contains the electron density maps of POPE bilayers at three different RH's calculated from the structure factors shown in Figure 6a. Notice that these differ mainly in the separation of the phosphocholine headgroups. This makes physical sense, since the amount of water is being increased and the bilayers do not undergo any phase transitions; the expected change would be an enlarged water region. In addition, the diffraction patterns of the dehydrated L_β phase POPE at 20 °C do not contain the extra nonlamellar reflection that the same phase bilayers had at 30 °C and 100% RH. It

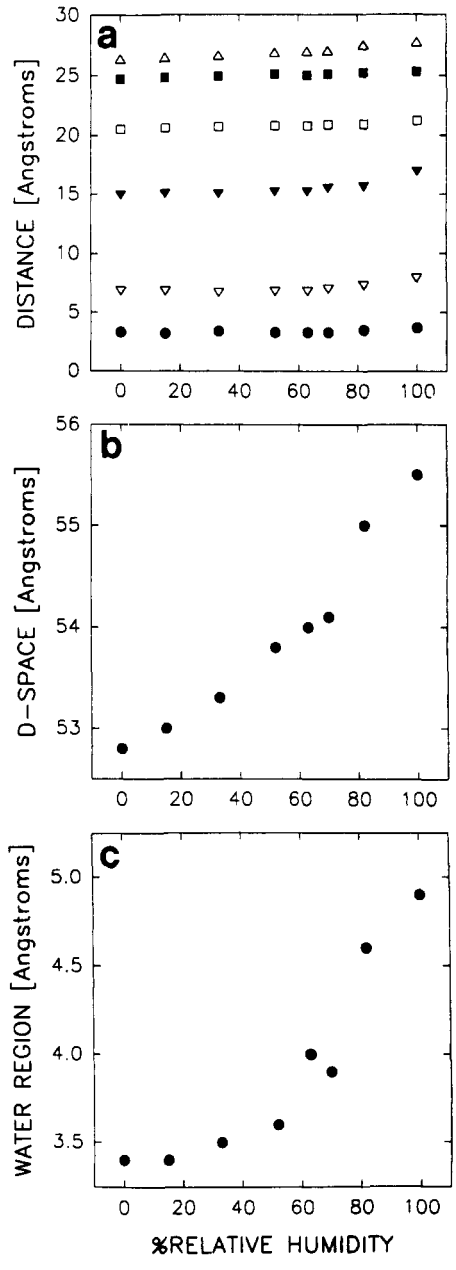

FIGURE 8: Relative humidity dependence at 20 °C of (a) the quasimolecular fragments (please refer to Figure 1) characterizing the structure of partially dehydrated L_β phase POPE [(●) 1; (▽) 2; (▼) 3; (□) 4; (■) 5; (△) 6], (b) the *d*-spacing in POPE bilayers, and (c) the water region (two times the difference between quasimolecular fragments 5 and 6).

is also interesting to note that, with increasing levels of hydration, the electron density profiles seem to get "smoother", losing some of the fine detail. This is especially prominent in the region between the peaks due to the backbone (COOH groups) and the phosphocholine headgroup [PO_4^-] (Figure 7). As pointed out earlier, this is indirect proof of less water being present in the partially dehydrated L_β POPE bilayers compared to the L_β bilayers at 20 °C or less (Figure 4).

In Figure 8a we observe gradual but small changes in the positions of the quasimolecular fragments as a function of relative humidity. This is unlike the abrupt shift in quasimolecular fragment position at 30 °C of POPE bilayers undergoing partial dehydration (Figure 5a). More interesting is the fact that the changes in *d*-spacing as a function of relative humidity are almost totally accounted for by the changes of the water region (Figure 8b,c). It is of interest to note that besides providing positional information about the various lipid groups, the modeling of the X-ray diffraction patterns indirectly provided us with the correct phases since the lowest *R*-factors were obtained with phases that were deemed to be correct from the continuous Fourier transforms.

Number of Water Molecules per Lipid. Although the electron density distributions clearly demonstrate that, at 100% RH, POPE exists in two distinct L_β phases differing only in the amount of water between their lamellae, we also believe that a quantization of the amount of water is necessary. Using the formalism of Nagle and Wiener (1988), we were able to obtain such information. One POPE molecule contains 28 CH_2 groups having a volume of 26 Å^3 each, two CH_3 groups having a total volume of 90 Å^3, one double bond of volume 43 Å^3 (Wiener & White, 1992), and finally one headgroup of 252 Å^3. Therefore, the total volume of one POPE lipid in the L_β phase is approximately 1113 Å^3. Since the number of water molecules does not affect the average electron density to any great extent, we assigned zero water molecules to the two phases even though we know that the two phases differ in their levels of hydration. We also assigned a volume of 1113 Å^3 to both phases although intuitively one would expect the dehydrated phase to have a slightly smaller volume (5–10 Å^3). Regardless, these two effects average out, and we calculate an average electron density of 0.356 e^-/Å^3 for the two L_β phase lipids. In addition, the area of the lipid could be calculated by knowing the effective length of the lipid (center of Gaussians due to the methyl and headgroup). Since POPE at 20 and 30 °C has an effective length of 21.2 and 22.1 Å, respectively, at 100% RH, we calculate the area per lipid to be 52.5 Å^2 at 20 °C and 50.4 Å^2 at 30 °C. Finally, the total number of waters per lipid is obtained by multiplying the average electron density by the area per lipid and $d/2$, minus the electrons due to the lipid (396 e^-), and dividing by 10 (e^- H_2O), since there are 10 electrons per water molecule, resulting in 14.6 and 9.7 waters per lipid for the POPE samples at 20 and 30 °C, respectively. It is important to note that the number of water molecules in the two different phases can be calculated using different assumptions (e.g., smaller average electron density value), thus yielding slightly different values than those stated above. However, even in those cases the ratio of the number of waters in the two phases is nearly invariant at about 1.5. Finally, the number of water molecules per lipid in the dehydrated L_β phase agrees favorably with the water content calculated for diarachinoyl-PE by Seddon et al. (1984) using X-ray measurements.

Electron Density Profiles for POPC Bilayers. Under most circumstances, PC's are known to form lamellar phases. Although a PC headgroup differs from a PE in the replacement of three methyl groups by three hydrogen atoms, this seemingly minor substitution alters the character of the lipids to a great extent. Their affinity for water is one of the most cited differences between the two species [e.g., Jendrasiak et al. (1974)], and recently, Rand et al. (1988) have suggested that the chain packing of a lipid can to a certain degree affect the hydration forces and ultimately the headgroup hydration. It is therefore interesting to compare the electron density profiles of POPC and POPE bilayers.

Using an oriented POPC sample at 20 °C, we observe the bilayers existing in three distinct lamellar phases as a function of RH. At 0% RH, the POPE bilayers form an L_δ phase; from approximately 15 to 50% RH the bilayers exist in an L_β phase and thereafter in an L_α phase. The diffraction pattern of the L_δ phase POPC bilayers (54.7 Å, not shown), besides containing the usual meridional reflections (commonly referred to as the small-angle reflections), also exhibits Bragg reflections

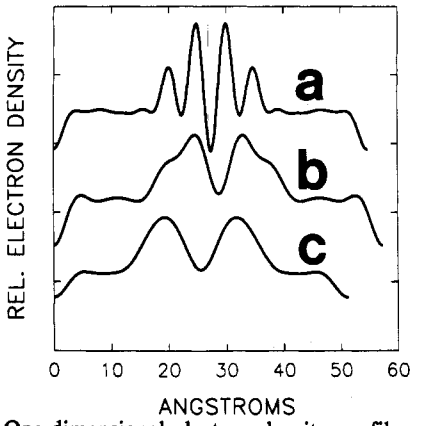

FIGURE 9: One-dimensional electron density profiles of oriented POPC bilayers at 20 °C. Panels: (a) L_δ phase bilayers at 0% RH having a *d*-spacing of 54.7 Å; 9b) L_β phase bilayers at 40% RH having a *d*-spacing of 57.4 Å; (c) L_α phase bilayers at 100% RH having a *d*-spacing of 51.2 Å. The corrected structure factors for L_δ phase POPC are −6392, 1253, −1425, −2549, 0, −1544, 0, −2249, 2283, −4625, 4009, −3658, 1793, and −687. For the L_β phase, the corrected structure factors are −6321, 429, 0, −3228, 562, −1728, 0, −1658, 479, and −574. For the L_α POPC bilayers the structure factors are given in Figure 10.

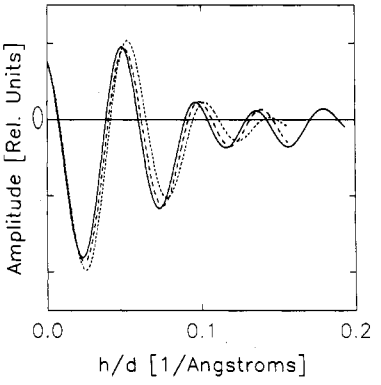

FIGURE 10: Continuous Fourier transforms of L_α phase POPC bilayers at 20 °C and RH's of 70% (—), 80% (– –), and 100% (···) having *d*-spacings of 51.7, 51.2, and 51.2 Å, respectively. The corrected structure factors are −5098, 325, 546, −3046, 695, −1102, 355, −1034, 262, and −273 for the 70% RH bilayers, −4765, −292, 971, −2982, 667, −955, 349, and −825 for the 80% RH bilayers, and −4644, −925, 1879, −2787, 395, −523, −128, and −224 for the 100% RH bilayers.

parallel to the meridional axis at inverse lattice spacings of 1/6.6 and 1/4.7 $Å^{-1}$ ($1:2^{1/2}:4^{1/2}$ etc.) as a result of the phosphocholine headgroups forming a two-dimensional square lattice of edge $\simeq$6.6 Å. In addition, the hydrocarbon chains in the L_δ phase have an orthorhombic packing arrangement as indicated by an equatorially centered reflection at a distance of 1/4.4 $Å^{-1}$ (Small, 1984; Ruocco & Shipley, 1982).

The one-dimensional electron density map of the L_δ phase of POPC is presented in Figure 9a. The peaks attributed to the backbone and headgroups are distinctly sharp and narrow as a result of the headgroups forming a lattice. The electron density map and indeed the diffraction pattern due to the L_δ phase of POPC bilayers are unlike any of the others in this study. However, the electron density profile for the L_β phase of POPC bilayers, having a *d*-spacing of 57.4 Å at 40% RH (Figure 9b), resembles those for POPE bilayers in the same phase as shown in Figure 4a. This is of interest since, as mentioned previously, PC's generally form lamellar phases and PE's are known to form both lamellar and hexagonal phases. Thus the stable bilayers of the more hydrated L_β phase of POPE (Figure 4a) closely correspond to the lamellar L_β phase of POPC (Figure 9b). The unique properties of

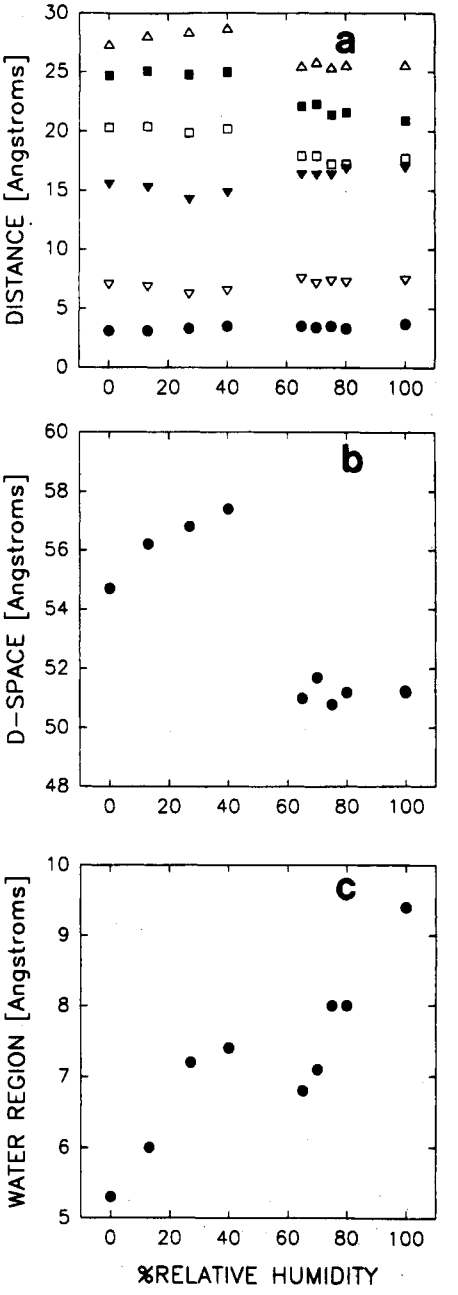

FIGURE 11: Relative humidity dependence at 20 °C of (a) the quasimolecular fragments (please refer to Figure 1) characterizing the structure of L_δ phase (0% RH), L_β phase (15–40% RH), and L_α phase (65–100% RH) POPC [(●) 1; (▽) 2; (▼) 3; (□) 4; (■) 5; (△) 6], (b) the *d*-spacing in POPC bilayers, and (c) the water region (two times the difference between quasimolecular fragments 5 and 6).

POPE are only observed in the partially dehydrated L_β phase (Figure 4b), which eventually lead to the formation of the hexagonal phase. Finally around 65% RH, the L_β POPC bilayers undergo a phase transition to the L_α phase (Figure 9c). Unlike the gel phases of POPE and POPC, the motif of the L_α phase POPC does change with increasing levels of hydration. This phenomenon is easily observed in the reconstruction of the continuous Fourier transforms of these bilayers (Figure 10). The transforms systematically expand outward with increasing levels of hydration, and in addition, they can be used to predict the correct signs for the structure factors (Torbet & Wilkins, 1976).

In Figure 11a, the gel-to-liquid-crystalline phase transition is clearly shown by the abrupt change in position of the quasimolecular fragments obtained by modeling the electron density profiles. It is interesting to note that the changes in

d-spacing as a function of relative humidity (Figure 11b) are not reflected in changes in the size of the water region (Figure 11c), unlike the POPE samples. From the above one can observe that the POPC and POPE bilayers are quite different in their phase behavior and hydration properties, but despite these differences both lipids exhibit similar structures in the hydrated L_β phase.

CONCLUSIONS

In this study we have attempted to provide some insight into the polymorphic tendencies of POPE and alluded to its possible metastable tendencies. X-ray diffraction patterns containing up to 14 orders were obtained for oriented POPE/water mixtures and POPC samples under a variety of conditions of temperature and hydration. The high-resolution (~4 Å) one-dimensional electron density profiles of POPE bilayers at various temperatures (5–50 °C) and constant relative humidity (100% RH) show that at low temperatures (5–20 °C), L_β phase POPE bilayers resemble those of POPC in the L_β phase and can undergo a lamellar-to-hexagonal phase transition only after they shed approximately one third of their water. An intermediate partially dehydrated L_β phase of POPE bilayers has been shown to exist both in a "pure phase" when in conditions far removed from an H_{II} phase transition and with another phase (eventually becomes an H_{II} phase) on approaching conditions favorable for H_{II} formation.

There has been considerable interest in recent years on the role of "hexagonal phase propensity" and its effect on membrane properties. There is increasing evidence that as membrane bilayers become more prone to enter the H_{II} phase, they can activate membrane-bound proteins such as protein kinase C (Epand, 1992) and rhodopsin (Gibson & Brown, 1993) as well as increase the rate of membrane fusion (Ellens et al., 1989). These changes in membrane function may not and probably do not require the actual formation of nonlamellar phases, even at low concentrations. The changes to the membrane's physical properties occur while the membrane remains in the lamellar phase. The physical changes in membrane bilayers which accompany increased hexagonal phase tendency while the membrane remains in the lamellar phase are not well understood. The present paper directly demonstrates the tendency of the lamellar phase to dehydrate as its hexagonal phase propensity increases with increasing temperature. Such a phenomenon is seen in the POPE bilayers, which can readily form the H_{II} phase, and not with the nonhexagonal-forming POPC bilayers.

ACKNOWLEDGMENT

J.K. thanks Dr. Erick J. Dufourc and Gerard Raffard for their many and various efforts since his arrival at Centre de Recherche Paul Pascal and Ms. Sarantia-Ann Katsaras for relevant discussions.

REFERENCES

Bagdassarian, C. K., Roux, D., Ben-Shaul, A., & Gelbart, W. M. (1991) *J. Chem. Phys. 94*, 3031–3041.
Boggs, J. M. (1987) *Biochim. Biophys. Acta 906*, 353–404.
Bryant, G., & Wolfe, J. (1989) *Eur. Biophys. J. 16*, 369–374.
Bryant, G., Pope, J. M., & Wolfe, J. (1992) *Eur. Biophys. J. 21*, 223–232.
Castresana, J., Nieva, J.-L., Rivas, E., & Alonso, A. (1992) *Biochem. J. 282*, 467–470.
Chang, H., & Epand, R. M. (1983) *Biochim. Biophys. Acta 728*, 319–324.
Chen, S. C., Sturtevant, J. M., & Gaffney, B. J. (1980) *Proc. Natl. Acad. Sci. U.S.A. 77*, 5060–5063.
Crowe, L. M., & Crowe, J. H. (1982) *Arch. Biochem. Biophys. 217*, 582.
Cullis, P. R., & De Kruijff, B. (1979) *Biochim. Biophys. Acta 559*, 399–420.
Dorset, D. L. (1990) *Biophys. J. 58*, 1077–1087.
Dorset, D. L. (1991a) *Biophys. J. 60*, 1356–1365.
Dorset, D. L. (1991b) *Biophys. J. 58*, 1366–1373.
Ellens, H., Siegel, D. P., Alford, D., Yeagle, P. L., Boni, L., Lis, L. J., Quinn, P. J., & Bentz, J. (1989) *Biochemistry 28*, 3692–3703.
Epand, R. M. (1990) *Chem. Phys. Lipids 52*, 227–230.
Epand, R. M. (1991) in *Cell and Model Membrane Interactions* (Ohki, S., Ed.) pp 135–147, Plenum Press, New York.
Epand, R. M. (1992) in *Protein Kinase C: Current Concepts and Future Perspectives* (Lester, D. S., & Epand, R. M., Eds.) pp 135–156, Ellis Horwood Ltd., Chichester, England.
Franks, N. P. (1976) *J. Mol. Biol. 100*, 345–358.
Gawrisch, K., Parsegian, V. A., Hajduk, D. A., Tate, M. W., Gruner, S. M., Fuller, N. L., & Rand, R. P. (1992) *Biochemistry 31*, 2856–2864.
Gibson, N. J., & Brown, M. F. (1993) *Biochemistry 32*, 2438–2454.
Gordon-Kamm, W. J., & Steponkus, P. L. (1984) *Proc. Natl. Acad. Sci. U.S.A. 81*, 6373–6377.
Jendrasiak, G. L., & Hasty, J. H. (1974) *Biochim. Biophys. Acta 337*, 79–91.
Katsaras, J., & Stinson, R. H. (1990) *Biophys. J. 57*, 649–655.
Katsaras, J., Stinson, R. H., Davis, J. H., & Kendall, E. J. (1991) *Biophys. J. 59*, 645–653.
Mantsch, H. H., Hsi, S. C., Butler, K. W., & Cameron, D. G. (1983) *Biochim. Biophys. Acta 728*, 325–330.
Marsh, D., & Seddon, J. M. (1982) *Biochim. Biophys. Acta 690*, 117–123.
McIntosh, T. J., & Simon, S. A. (1986) *Biochemistry 25*, 4948–4952.
Nagle, J. F., & Wiener, M. C. (1988) *Biochim. Biophys. Acta 942*, 1–10.
Press, W. H., Flannery, B. P., Teukolsky, S. A., & Vetterling, W. T. (1992) *Numerical Recipes in C. The Art of Scientific Computing*, 2nd ed., p 408, Cambridge University Press, Cambridge, U.K.
Rand, R. P., Fuller, N., Parsegian, V. A., & Rau, D. C. (1988) *Biochemistry 27*, 7711–7722.
Ruocco, M. J., & Shipley, G. G. (1982) *Biochim. Biophys. Acta 684*, 59–66.
Sayre, D. (1952) *Acta Crystallogr. B5*, 843.
Seddon, J. M., Cevc, G., Kaye, R. D., & Marsh, D. (1984) *Biochemistry 23*, 2634–2644.
Shannon, C. E. (1949) *Proc. Inst. Radio Eng. N.Y. 37*, 10–21.
Small, D. M. (1984) *J. Lipid Res. 25*, 1490–1500.
Torbet, J., & Wilkins, M. H. F. (1976) *J. Theor. Biol. 62*, 447–458.
Webb, M. S., Hui, S. W., & Steponkus, P. L. (1993) *Biochim. Biophys. Acta 1145*, 93–104.
Wiener, M. C., & White, S. H. (1991) *Biophys. J. 59*, 174–185.
Wiener, M. C., & White, S. H. (1992) *Biophys. J. 61*, 434–447.
Wiener, M. C., King, G. I., & White, S. H. (1991) *Biophys. J. 60*, 568–576.
Wilkinson, D. A., & Nagle, J. F. (1981) *Biochemistry 20*, 187–192.